

Deconfinement and Chiral Symmetry Restoration in a Strong Magnetic Background

Raoul Gatto^{1,*} and Marco Ruggieri^{2,†}

¹*Departement de Physique Theorique, Universite de Geneve, CH-1211 Geneve 4, Switzerland*

²*Yukawa Institute for Theoretical Physics, Kyoto University, Kyoto 606-8502, Japan*

We perform a model study of deconfinement and chiral symmetry restoration in a strong magnetic background. We use a Nambu-Jona Lasinio model with the Polyakov loop, taking into account a possible dependence of the coupling on the Polyakov loop expectation value, as suggested by the recent literature. Our main result is that, within this model, the deconfinement and chiral crossovers of QCD in strong magnetic field are entangled even at the largest value of eB considered here, namely $eB = 30m_\pi^2$ (that is, $B \approx 6 \times 10^{15}$ Tesla). The amount of split that we measure is, at this value of eB , of the order of 2%. We also study briefly the role of the 8-quark term on the entanglement of the two crossovers. We then compare the phase diagram of this model with previous results, as well as with available Lattice data.

PACS numbers: 12.38.Aw, 12.38.Mh

Keywords: Hot quark matter, Effective models of QCD, Deconfinement and chiral symmetry restoration in magnetic fields.

I. INTRODUCTION

The study of the Quantum Chromodynamics (QCD) vacuum, and of its modifications under the influence of external factor like temperature, baryon chemical potential, external fields, is one of the most attractive topics of modern physics. One of the best strategies to overcome the difficulty to study chiral symmetry breaking and deconfinement, which share a non-perturbative origin, is offered by Lattice QCD simulations at zero chemical potential [1–5]. At vanishing quark chemical potential, it is established that two crossovers take place in a narrow range of temperature; one for quark deconfinement, and another one for the (approximate) restoration of chiral symmetry. Besides, the use of the Schwinger-Dyson equations for the quark self-energy [6, 7], and the use of functional renormalization group [8] to the Hamiltonian formulation of Yang-Mills theory in Coulomb gauge, are very promising [9, 10]. QCD with one quark flavor at finite temperature and quark chemical potential has been considered in [11] within the functional renormalization group approach, combined with re-bosonization techniques; in [12], the renormalization group flow of the Polyakov-Loop potential and the flow of the chiral order parameter have been computed. The results of [12] suggest that the chiral and deconfinement phase transition temperature agree within a few MeV for vanishing and (small) quark chemical potentials. Furthermore, an interesting possibility to map solutions of the Yang-Mills equations of motion with those of a scalar field theory has been proved in [13].

An alternative approach to the physics of strong interactions, which is capable to capture some of the non-perturbative properties of the QCD vacuum, is the Nambu-Jona Lasinio (NJL) model [14], see Refs. [15] for

reviews. In this model, the QCD gluon-mediated interactions are replaced by effective interactions among quarks, which are built in order to respect the global symmetries of QCD. Beside this, the parameters of the model are fixed to reproduce some phenomenological quantity of the QCD vacuum; therefore, it is reasonable that the main characteristics of its phase diagram represent, at least qualitatively, those of QCD.

In recent years, the NJL model has been improved in order to be capable to compute quantities which are related to the confinement-deconfinement transition of QCD. It is well known that color confinement can be described in terms of the center symmetry of the color gauge group and of the Polyakov loop [16], which is an order parameter for the center symmetry in the pure gauge theory. In theories with dynamical fermions, the Polyakov loop is still a good indicator for the confinement-deconfinement transition, as suggested by Lattice data at zero chemical potential [1–5]. Motivated by this property, the Polyakov extended Nambu-Jona Lasinio model (P-NJL model) has been introduced [17, 18], in which the concept of statistical confinement replaces that of the true confinement of QCD, and an effective potential describing interaction among the chiral condensate and the Polyakov loop is achieved by the coupling of quarks to a background temporal gluon field, and then integrating over quark fields in the partition function. The P-NJL model, as well as its renormalizable extension, namely the Polyakov extended Quark-Meson model (P-QM), have been studied extensively in many contexts [19–36].

In a remarkable paper [37] it has been shown by Kondo that it is possible to derive the effective 4-quark interaction of the NJL model, starting from the QCD lagrangian. In his derivation, Kondo has shown explicitly that the NJL vertex has a non-local structure, that is, it is momentum-dependent; besides, the vertex acquires a non-trivial dependence on the phase of the Polyakov loop. This idea has been implemented within the P-NJL model

* raoul.gatto@unige.ch

† ruggieri@yukawa.kyoto-u.ac.jp

in [31]; the modified model has then been named EPNJL, and the Polyakov-loop-dependent vertex has been called entanglement vertex. We will make use of this nomenclature in the present article. Before going ahead, it is worth to notice that a low-energy limit of QCD, leading to the non-local Nambu-Jona-Lasinio model studied in [38], has been discussed independently in [39]. In this reference, the low-energy limit of the gluon propagator leads to a relation among the NJL coupling constant and the string tension.

In this article, we report on our study of deconfinement and chiral symmetry restoration at finite temperature in a strong magnetic background. This study is motivated by several reasons. Firstly, it is extremely interesting to understand how an external field can modify the main characteristics of confinement and spontaneous chiral symmetry breaking. Lattice studies on QCD in magnetic (as well as chromo-magnetic) backgrounds can be found in [40–42]. Studies of QCD in magnetic fields, and of QCD-like theories as well, can be found in Refs. [43–50]. Besides, strong magnetic fields might be produced in non-central heavy ion collisions [51, 52]. More concretely, at the center-of-mass energy reachable at LHC, $\sqrt{s_{NN}} \approx 4.5$ TeV, the magnetic field can be as large as ¹ $eB \approx 15m_\pi^2$ according to [52]. It has been argued that in these conditions, the sphaleron transitions of finite temperature QCD, give rise to Chiral Magnetic Effect (CME) [51, 53].

The novelty of this study is the use of the EPNJL model in our calculations, in the one-loop approximation. In comparison with the original PNJL model of [18], the EPNJL model has two additional parameters. However, they are fixed from the QCD thermodynamics at zero magnetic field, as we will discuss in more detail later. Therefore, the results at a finite value of the magnetic field strength have to be considered as predictions of the model. Our main result is that the entanglement of the NJL coupling constant and the Polyakov loop, might affect crucially the phase diagram in the temperature/magnetic field strength plane. Previous model studies [43–45] have revealed that both the deconfinement temperature, T_L , and the chiral symmetry restoration temperature, T_χ , are enhanced by a magnetic field, in agreement with the Lattice data of Ref. [40]. The model results are in slight disagreement with the Lattice, in the sense that the former predict a considerable split of T_L and T_χ as the strength of the magnetic field is increased. Within the EPNJL model, we can anticipate one of the results, that is, the split among T_L and T_χ might be considerably reduced even at large values of the magnetic field strength. In particular, using the values of the parameters of [31], which arise from a best-fit of Lattice data at zero and imaginary chemical potential and which

are appropriate for our study, we find a split of the order of 2% at the largest value of eB considered, namely $eB = 30m_\pi^2$.

In [45] a similar computation within a model without entanglement, but with an 8-quark interaction added, has been performed. Following the nomenclature of [31], we call the latter model, PNJL₈ model. We find the comparison among the EPNJL and the PNJL₈ models very instructive. As a matter of fact, the parameters in the two models are chosen to reproduce the QCD thermodynamics at zero and imaginary chemical potential [28, 31]. Therefore, both of them are capable to describe QCD in the same regime. It is interesting that, because of the different interactions content, the two models predict a slight different behavior of hot quark matter in strong magnetic field. In the next future, the comparison with refined Lattice data can enlighten on which of the two models is a more faithful description of QCD.

The paper is organized as follows: in Section II we summarize the formalism: we derive the quark propagator and the equation for the chiral condensates in magnetic field, within the EPNJL model, in the one-loop approximation; then, we compute the thermodynamic potential. In Section III, we collect our results for the chiral condensate and the expectation value of the Polyakov loop, for several values of the magnetic field strength. In Section IV, we briefly investigate on the effect of the 8-quark interaction in the EPNJL model in magnetic field. In Section V, we draw the phase diagram of the EPNJL model in magnetic field, and make a comparison with our previous result [45]. Finally, in Section VI we draw our conclusions, and briefly comment on possible extensions and prosecutions of our study.

We use natural units throughout this paper, $\hbar = c = k_B = 1$, and work in Euclidean space-time $R^4 = \beta V$, where V is the volume and $\beta = 1/T$ with T corresponding to the temperature of the system. Moreover, we take a non-zero current quark mass. In this case, both deconfinement and chiral symmetry breaking are crossovers; however, we sometimes will make use of the term “phase transition” to describe them, for stylistic reasons. It should be clear from the context that our “phase transitions” are meant to be crossovers unless stated differently.

II. THE MODEL WITH ENTANGLEMENT VERTEX

We consider a model in which quark interaction is described by the following lagrangian density:

$$\mathcal{L} = \bar{\psi} (i\gamma^\mu D_\mu - m) \psi + \mathcal{L}_I ; \quad (1)$$

here ψ is the quark Dirac spinor in the fundamental representation of the flavor $SU(2)$ and the color group; τ correspond to the Pauli matrices in flavor space. A sum over color and flavor is understood. The covariant derivative

¹ In this article, we measure eB in units of the vacuum squared pion mass m_π^2 ; then, $eB = m_\pi^2$ corresponds to $B \approx 2 \times 10^{14}$ Tesla.

embeds the QED coupling of the quarks with the external magnetic field, as well as the QCD coupling with the background gluon field which is related to the Polyakov loop, see below. Furthermore, we have defined

$$\mathcal{L}_I = G \left[(\bar{\psi}\psi)^2 + (i\bar{\psi}\gamma_5\tau\psi)^2 \right] ; \quad (2)$$

This interaction term is invariant under $SU(2)_V \otimes SU(2)_A \otimes U(1)_V$. In the chiral limit, this is the symmetry group of the action as well, if no magnetic field is applied. However, this group is broken explicitly to $U(1)_V^3 \otimes U(1)_A^3 \otimes U(1)_V$ if the magnetic field is coupled to the quarks, because of the different electric charge of u and d quarks. Here, the superscript 3 in the V and A groups denotes the transformations generated by τ_3 , $\tau_3\gamma_5$ respectively. Therefore, the chiral group in presence of a magnetic field is $U(1)_V^3 \otimes U(1)_A^3$. This group is then explicitly broken by the quark mass term to $U(1)_V^3$.

We are interested to the interplay among chiral symmetry restoration and deconfinement in a strong magnetic field. To compute a temperature for the deconfinement crossover, we use the expectation value of the Polyakov loop, that we denote by L . In order to compute L we introduce a static, homogeneous and Euclidean background temporal gluon field, $A_0 = iA_4 = i\lambda_a A_4^a$, coupled minimally to the quarks via the QCD covariant derivative [18]. Then

$$L = \frac{1}{3} \text{Tr}_c \exp(i\beta\lambda_a A_4^a) , \quad (3)$$

where $\beta = 1/T$. In the Polyakov gauge, which is convenient for this study, $A_0 = i\lambda_3\phi + i\lambda_8\phi^8$; moreover, we work at zero quark chemical potential, therefore we can take $L = L^\dagger$ from the beginning, which implies $A_4^8 = 0$. This choice is also motivated by the study of [44], where it is shown that the paramagnetic contribution of the quarks to the thermodynamic potential induces the breaking of the Z_3 symmetry, favoring the configurations with a real-valued Polyakov loop (see Section III.C of [44] for an excellent discussion of this point). We have then [18, 19]

$$L = \frac{1 + 2\cos(\beta\phi)}{3} . \quad (4)$$

As already discussed in the Introduction, it has been shown that it is possible to derive the effective 4-quark interaction (2) starting from the QCD lagrangian [37]. In [37] it has been shown that the NJL vertex has a non-local structure, that is, it is momentum-dependent. An analogous conclusion is achieved in [39]. More important for our study, the NJL vertex acquires a non-trivial dependence on the phase of the Polyakov loop. Therefore, in the model we consider here, it is important to keep into account this dependence. The exact dependence of G on L has not yet been computed; it is possible that it will be determined in the next future by means of the functional renormalization group approach [37]. In our

study, we follow a more phenomenological approach to the problem, using the ansatz introduced in [31], that is

$$G = g \left[1 - \alpha_1 L \bar{L} - \alpha_2 (L^3 + \bar{L}^3) \right] , \quad (5)$$

and we take $L = \bar{L}$ from the beginning. The functional form in the above equation is constrained by C and extended Z_3 symmetry. We refer to [31] for a more detailed discussion. The numerical values of α_1 and α_2 have been fixed in [31] by a best fit of the available Lattice data at zero and imaginary chemical potential of Ref. [54], which have been confirmed recently in [55]. In particular, the fitted data are the critical temperature at zero chemical potential, and the dependence of the Roberge-Weiss endpoint on the bare quark mass.

The values $\alpha_1 = \alpha_2 \equiv \alpha = 0.2 \pm 0.05$ have been obtained in [31] using a hard cutoff regularization scheme. We will focus mainly on the case $\alpha = 0.2$ as in [31]. We have verified that in our regularization scheme, our results are in quantitative agreement with those of [31], when we take the parameter $T_0 = 190$ MeV in the Polyakov loop effective potential in agreement with [31], see below. Then, we will study how the results change when we vary α .

A. Quark propagator and chiral condensate in magnetic field

We work in the mean field approximation throughout this paper, neglecting pseudoscalar condensates; moreover, we make the assumption that condensation takes place only in the flavor channels τ_0 and τ_3 . The mean field interaction term Eq. (2) can be cast in the form

$$\mathcal{L} = -2G\Sigma (\bar{u}u + \bar{d}d) - G\Sigma^2 , \quad (6)$$

where $\Sigma = -\langle \bar{u}u + \bar{d}d \rangle$.

In a magnetic field, the chiral condensates of u and d quarks have to be different, because the electric charges of these quarks are different. Even if the one-loop quark self-energies in Eq. (6) depend on the sum of the two condensates, being therefore flavor independent, it is straightforward to show that the two condensates turn out to be different, by taking the trace of the propagator of the two quarks. The interaction (6) is diagonal in flavor space, therefore we can focus on the propagator of a single flavor f .

To write the quark propagator we use the Ritus method [56], which allows to expand the propagator on the complete and orthonormal set made of the eigenfunctions of a charged fermion in a homogeneous and static magnetic field. This is a well known procedure, discussed many times in the literature, see for example [57–60]; therefore it is enough to quote the final result,

$$S_f(x, y) = \sum_{k=0}^{\infty} \int \frac{dp_0 dp_2 dp_3}{(2\pi)^4} E_P(x) \Lambda_k \frac{1}{\not{P} \cdot \gamma - M} \bar{E}_P(y) , \quad (7)$$

where $E_P(x)$ corresponds to the eigenfunction of a charged fermion in magnetic field, and $\bar{E}_P(x) \equiv \gamma_0(E_P(x))^\dagger \gamma_0$. In the above equation,

$$P = (p_0 + iA_4, 0, \mathcal{Q}\sqrt{2k|Q_f eB|}, p_z), \quad (8)$$

where $k = 0, 1, 2, \dots$ labels the k^{th} Landau level, and $\mathcal{Q} \equiv \text{sign}(Q_f)$, with Q_f denoting the charge of the flavor f ; Λ_k is a projector in Dirac space which keeps into account the degeneracy of the Landau levels; it is given by

$$\Lambda_k = \delta_{k0} [\mathcal{P}_+ \delta_{\mathcal{Q},+1} + \mathcal{P}_- \delta_{\mathcal{Q},-1}] + (1 - \delta_{k0})I, \quad (9)$$

where \mathcal{P}_\pm are spin projectors and I is the identity matrix in Dirac spinor indices. The propagator in Eq. (7) has a non-trivial color structure, due to the coupling to the background gauge field, see Eq. (8).

The trace of the f -quark propagator is minus the chiral condensate $\langle \bar{f}f \rangle$, with $f = u, d$. Taking the trace in coordinate and internal space, it is easy to show that the following equation holds:

$$\langle \bar{f}f \rangle = -N_c \frac{|Q_f eB|}{2\pi} \sum_{k=0}^{\infty} \beta_k \int \frac{dp_z}{2\pi} \frac{M_f}{\omega_f} \mathcal{C}(L, \bar{L}, T|p_z, k). \quad (10)$$

Here,

$$\mathcal{C}(L, \bar{L}, T|p_z, k) = U_\Lambda - 2\mathcal{N}(L, \bar{L}, T|p_z, k), \quad (11)$$

and \mathcal{N} denotes the statistically confining Fermi distribution function,

$$\mathcal{C}(L, \bar{L}, T|p_z, k) = \frac{1 + 2Le^{\beta\omega_f} + Le^{2\beta\omega_f}}{1 + 3Le^{\beta\omega_f} + 3Le^{2\beta\omega_f} + e^{3\beta\omega_f}}, \quad (12)$$

where

$$\omega_f^2 = p_z^2 + 2|Q_f eB|k + M_f^2, \quad (13)$$

with

$$M_u = M_d = m_0 + 2G\Sigma. \quad (14)$$

The first and the second addenda in the r.h.s. of Eq. (10) correspond to the vacuum and the thermal fluctuations contribution to the chiral condensate, respectively. The coefficient $\beta_k = 2 - \delta_{k0}$ keeps into account the degeneracy of the Landau levels. The vacuum contribution is ultraviolet divergent. In order to regularize it, we adopt a smooth regulator U_Λ , which is more suitable, from the numerical point of view, in our model calculation with respect to the hard-cutoff which is used in analogous calculations without magnetic field. In this article we chose

$$U_\Lambda = \frac{\Lambda^{2N}}{\Lambda^{2N} + (p_z^2 + 2|Q_f eB|k)^N}. \quad (15)$$

To be specific, we consider here the case $N = 5$, for numerical convenience. A larger value of N increases the cutoff artifacts, as already discussed in detail in [43, 45, 47], but leaves the qualitative picture unchanged; on the other hand, a smaller value of N , namely $N \leq 3$, makes not possible the fit of the pion decay constant and of the chiral condensate in the vacuum. The (more usual) 3-momentum cutoff regularization scheme is recovered in the limit $N \rightarrow \infty$; we notice that, even if the choice $N = 5$ may seem arbitrary to some extent, it is not more arbitrary than the choice of the hard cutoff, that is, of a regularization scheme.

By virtue of Eq. (10) it is easy to argue that the condensates of u and d quarks are different in magnetic field. As a matter of fact, the different value of the charges makes the r.h.s. of the above equation flavor-dependent, even if Σ is flavor-singlet. Once we compute the mean field value of Σ by minimization of the thermodynamic potential (see the next Section), we will use Eq. (10) to evaluate the chiral condensates for u and d quarks in magnetic field.

B. Thermodynamic potential

In the one-loop approximation, the thermodynamic potential Ω is given by

$$\Omega = \mathcal{U}(L, \bar{L}, T) + G\Sigma^2 - \frac{1}{\beta V} \text{Tr} \log(\beta S^{-1}), \quad (16)$$

where the trace is over color, flavor, Dirac and space-time indices and the propagator for each flavor is given by Eq. (7). It is straightforward to derive the final result, namely

$$\begin{aligned} \Omega &= \mathcal{U}(L, \bar{L}, T) + U_M \\ &- \sum_{f=u,d} \frac{|Q_f eB|}{2\pi} \sum_k \beta_k \int_{-\infty}^{+\infty} \frac{dp_z}{2\pi} \mathcal{G}(L, \bar{L}, T|p_z, k). \end{aligned} \quad (17)$$

In the above equation, the first line corresponds to the classical contribution; we have defined

$$U_M = G_S \Sigma^2; \quad (18)$$

the second line corresponds to the sum of vacuum and thermal one loop contributions, respectively, and arise after integration over the fermion fluctuations in the functional integral. We have defined

$$\mathcal{G}(L, \bar{L}, T|p_z, k) = N_c U_\Lambda(\mathbf{p}) \omega_f + \frac{2}{\beta} \log \mathcal{F}, \quad (19)$$

with

$$\mathcal{F}(L, \bar{L}, T|p_z, k) = 1 + 3Le^{-\beta\omega_f} + 3\bar{L}e^{-2\beta\omega_f} + e^{-3\beta\omega_f}. \quad (20)$$

The potential term $\mathcal{U}[L, \bar{L}, T]$ in Eq. (17) is built by hand in order to reproduce the pure gluonic lattice data [19, 20]. We adopt the following logarithmic form [20],

$$\mathcal{U}[L, \bar{L}, T] = T^4 \left\{ -\frac{a(T)}{2} \bar{L}L + b(T) \ln[1 - 6\bar{L}L + 4(\bar{L}^3 + L^3) - 3(\bar{L}L)^2] \right\}, \quad (21)$$

with three model parameters (one of four is constrained by the Stefan-Boltzmann limit),

$$\begin{aligned} a(T) &= a_0 + a_1 \left(\frac{T_0}{T} \right) + a_2 \left(\frac{T_0}{T} \right)^2, \\ b(T) &= b_3 \left(\frac{T_0}{T} \right)^3. \end{aligned} \quad (22)$$

The standard choice of the parameters reads $a_0 = 3.51$, $a_1 = -2.47$, $a_2 = 15.2$ and $b_3 = -1.75$. The parameter T_0 in Eq. (21) sets the deconfinement scale in the pure gauge theory. In absence of dynamical fermions one has $T_0 = 270$ MeV. However, dynamical fermions induce a dependence of this parameter on the number of active flavors [33]. For the case of two light flavors to which we are interested here, we take $T_0 = 212$ MeV as in [45].

As a final remark, it is easy to show that summing Eq. (10) for u and d quarks, one reproduces the equation satisfied by Σ , the latter being obtained from the stationarity condition $\partial\Omega/\partial\Sigma = 0$.

III. DECONFINEMENT AND CHIRAL SYMMETRY RESTORATION

In this Section we summarize our numerical results. In this study we fix the values of g , Λ and m_0 to reproduce the values of f_π and m_π in the vacuum, as well as the numerical value of the light quarks chiral condensate. We have then $\Lambda = 626.76$ MeV, $g = 2.02/\Lambda^2$. The pion mass in the vacuum, $m_\pi = 139$ MeV, is used to fix the numerical value of the bare quark mass via the GMOR relation $f_\pi^2 m_\pi^2 = -2m_0 \langle \bar{u}u \rangle$; this gives $m_0 = 5$ MeV when we take $\langle \bar{u}u \rangle = (-253 \text{ MeV})^3$. Finally, we take $T_0 = 212$ MeV in the Polyakov loop effective potential as in [45], unless stated differently. The values of Σ and L are computed by the minimization of the thermodynamic potential.

A. The case $\alpha_1 = \alpha_2 = 0.2$

In Fig. 1 we plot our data for the chiral condensate Σ , measured in units of the condensate at $T = eB = 0$, that is $\Sigma_0 = 2 \times (-253 \text{ MeV})^3$, and the expectation value of the Polyakov loop as a function of temperature, computed for several values of the magnetic field strength.

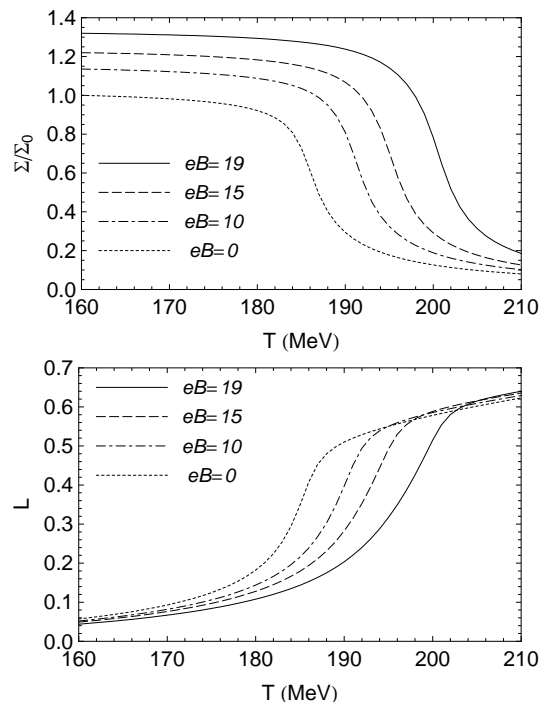


FIG. 1. *Upper panel:* Chiral condensate Σ , measured in units of the chiral condensate at zero temperature and zero field, Σ_0 , as a function of temperature, for several values of the magnetic field strength. *Lower panel:* Expectation value of the Polyakov loop, L , as a function of temperature, for several values of the magnetic field strength. The data are obtained for $\alpha = 0.2$. In the figures, the magnetic fields are measured in units of m_π^2 .

They are computed from the minimization of the thermodynamic potential in Eq. (17). In the numerical computation, we have chosen $\alpha_1 = \alpha_2 \equiv \alpha = 0.2$ as in [31].

The results shown in Fig. 1 are interesting for several reasons. Firstly, if we identify the deconfinement crossover with the temperature T_L at which dL/dT is maximum, and the chiral crossover with the temperature T_χ at which $|d\Sigma/dT|$ is maximum, we observe that the two temperatures are very close also in a strong magnetic field. For concreteness, at $eB = 0$ we find $T_P = T_\chi = 185.5$ MeV. Besides, at $eB = 19m_\pi^2$ we find $T_P = 199$ MeV and $T_\chi = 201$ MeV. Hence at the strongest value of eB considered here, namely $eB = 19m_\pi^2$, the entanglement vertex makes the split of the two crossovers of $\approx 1.5\%$. From the model point of view, it is easy to understand why deconfinement and chiral symmetry restoration are entangled also in strong magnetic field. As a matter of fact, using the data shown in Fig. 1, it is possible to show that the NJL coupling constant in the pseudo-critical region in this model decreases of the 15% as a consequence of the deconfinement crossover. Therefore, the strength of the interaction responsible for the spontaneous chiral symmetry breaking is strongly affected by the deconfinement, with the obvious conse-

quence that the numerical value of the chiral condensate drops down and the chiral crossover takes place. We have verified that the picture remains qualitatively and quantitatively unchanged if we perform a calculation at $eB = 30m_\pi^2$. In this case, we find $T_L = 224$ MeV and $T_\chi = 225$ MeV.

Before going ahead, it is worth to notice that we have also considered the case $T_0 = 190$ MeV, which corresponds to the value considered in [31]. In this case, for $eB = 0$ we find $T_\chi = T_L = 175$ MeV, in excellent agreement with [31]. This result is comforting, because it shows that even using a different regularization scheme, the UV-regulator does not affect the physical predictions at $eB = 0$. Moreover, at $eB/m_\pi^2 = 30$, we find $T_\chi \approx T_L = 215$ MeV.

This result can be compared with our previous calculation [43] in which we did not include the Polyakov loop dependence of the NJL coupling constant. In [43] we worked in the chiral limit and we observed that the Polyakov loop crossover in the PNJL model is almost insensitive to the magnetic field; on the other hand, the chiral phase transition temperature was found to be very sensitive to the strength of the applied magnetic field, in agreement with the well known magnetic catalysis scenario [46]. This model prediction has been confirmed within the Polyakov extended quark-meson model in [44], when the contribution from the vacuum fermion fluctuations to the energy density is kept into account²; we then obtained a similar result in [45], in which we turned from the chiral to the physical limit at which $m_\pi = 139$ MeV, and introduced the 8-quark term as well (PNJL₈ model, according to the nomenclature of [31]). The comparison with the results of the PNJL₈ model of [45] is interesting because the model considered there, was tuned in order to reproduce the Lattice data at zero and imaginary chemical potential [28], like the model we use in this study. Therefore, they share the property to describe the QCD thermodynamics at zero and imaginary chemical potential; it is therefore instructive to compare their predictions at finite eB .

For concreteness, in [45] we found $T_P = 185$ MeV and $T_\chi = 208$ MeV at $eB = 19m_\pi^2$, corresponding to a split of $\approx 12\%$. On the other hand, in the present calculation we measure a split of $\approx 1.5\%$ at the largest value of eB considered. Therefore, the results of the two models are in slight quantitative disagreement; this disagreement is then reflected in a slightly different phase diagram. We will draw the phase diagram of the two models in a next Section; however, since now it is easy to understand what the main difference consists in: the PNJL₈ model predicts some window in the $eB - T$ plane in which chiral

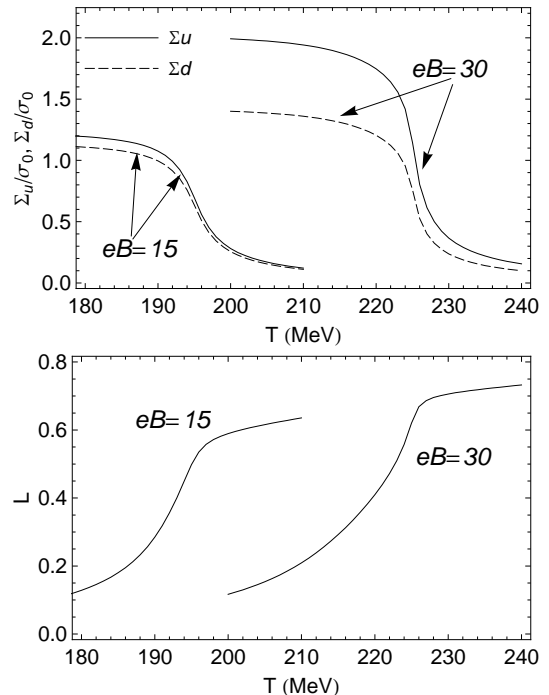


FIG. 2. *Upper panel:* Chiral condensates of u and d quarks as functions of temperatures in the pseudo-critical region, at $eB = 15m_\pi^2$ and $eB = 30m_\pi^2$. Condensates are measured in units of their value at zero magnetic field and zero temperature, namely $\sigma_0 = (-253 \text{ MeV})^3$. *Lower panel:* Polyakov loop expectation value as a function of temperature, at $eB = 15m_\pi^2$ and $eB = 30m_\pi^2$. Data correspond to $\alpha = 0.2$.

symmetry is still broken by a chiral condensate, but deconfinement already took place. In the case of the EPNJL model, this window is shrunk to a very small one, because of the entanglement of the two crossovers at finite eB . On the other hand, it is worth to stress that the two models share an important qualitative feature: both chiral restoration and deconfinement temperatures are enhanced by a strong magnetic field, in qualitative agreement with the existing Lattice data [40].

A further interesting feature of our data is that in the low temperature region, the Polyakov loop is suppressed as we increase the strength of the magnetic field; on the other hand, in the deconfinement phase, L is enhanced by the magnetic field. This result was also found in our previous studies [43, 45] with a fixed coupling constant; more remarkably, this result is in agreement with the Lattice data [40]. At the moment we do not have physical arguments to explain this result, but we agree with the authors of Ref. [40] that this aspect should be considered in more detail from the theoretical point of view.

For completeness, we plot in Fig 2 the chiral condensates of u and d quarks as a function of temperature, at $eB = 15m_\pi^2$ and $eB = 30m_\pi^2$. The condensates are measured in units of their value at zero magnetic field and zero temperature, namely $\sigma_0 \equiv \langle \bar{u}u \rangle = \langle \bar{d}d \rangle =$

² If the vacuum corrections are neglected, the deconfinement and chiral crossovers are found to be coincident even in very strong magnetic fields [44], but the critical temperature decreases as a function of eB ; this scenario is very interesting theoretically, but it seems it is excluded from the recent Lattice simulations [40].

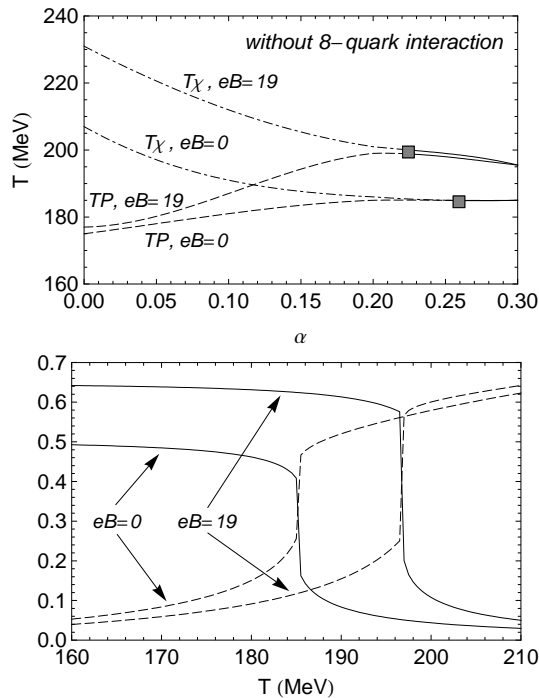


FIG. 3. *Upper panel:* pseudo-critical temperatures as functions of the parameter α in the NJL coupling constant. Dashed lines correspond to the Polyakov loop crossover, for $eB = 0$ and $eB = 19$. Dot-dashed lines correspond to the chiral crossover. The grey squares denote the value of α at which the crossover becomes a first-order phase transition. *Lower panel:* Polyakov loop expectation value (dashed lines) and half of $\Sigma(eB)/\Sigma(eB = 0)$ (solid lines) as functions of temperature, for $\alpha = 0.275$. In both panels the magnetic fields are measured in units of m_π^2 .

$(-253 \text{ MeV})^3$. They are computed by a two-step procedure: firstly we find the values of Σ and L that minimize the thermodynamic potential; then, we make use of Eq. (10) to compute the expectation values of $\bar{u}u$ and $\bar{d}d$ in magnetic field. If we measure the strength of the crossover by the value of the peak of $|d\Sigma/dT|$, it is obvious from the Figure that the chiral crossover becomes stronger and stronger as the strength of the magnetic field is increased, in agreement with [40].

B. Varying α

Since our study is based on a simple model, and we can not compute the exact values of the parameter α in Eq. (5) starting from first principles, we find very instructive to measure the robustness of our results as we vary the numerical value of this parameter. We emphasize that in [31] an estimate for the numerical value of α is achieved via the best fit of the model data with the Lattice data at zero and imaginary chemical potential. However, in that reference a different regularization

scheme is used. Therefore, we can expect that a slightly different value of α is needed in our case. However, it is useful to observe that in the limit of zero field, our regulator is very similar, quantitatively speaking, to the hard-cutoff of [31], because of the strong power-law decay of U_Λ as $|p| \approx \Lambda$. Therefore, the possible numerical deviation in the parameters is expected to be very tiny, if any. We have a further corroboration we are on target with parameters: if we chose $T_0 = 190 \text{ MeV}$ as in [31], we find $T_\chi = T_L = 175 \text{ MeV}$, in quantitative agreement with [31]; this convinces that our ultraviolet regulator does not lead to quantitative discrepancy with [31] at zero magnetic field.

We have investigated the dependence of the pseudo-critical temperatures as a function of α , at $eB = 0$ and $eB = 19m_\pi^2$. The results of our computations are collected in the upper panel of Fig. 3. At $\alpha = 0$, which corresponds to the original PNJL model, we measure a split of the two critical temperatures of $\approx 18\%$ even at $eB = 0$. This is well known result in the PNJL literature [19, 20], and to overcome this problem, several solutions have been suggested, like the use of the 8-quark interaction [24, 31]. However, the discrepancy of the critical temperatures is enhanced as the value of eB is increased. At $eB = 19m_\pi^2$ we find a split of $\approx 30\%$. As we increase α , the two temperatures get closer rapidly, both at zero and at non-zero value of the magnetic field strength. At $\alpha = 0.2$, which is the result that we have discussed previously and is the value quoted in [31], the two temperatures are almost coincident.

An interesting point that we have found is that increasing further the value of α , the crossovers become stronger and stronger; there exists a critical value of α at which the crossover is replaced by a sudden jump in the chiral condensate and in the Polyakov loop expectation value. This value of α is denoted by a green square in Fig. 3, and it is eB -dependent. For concreteness, in the lower panel of Fig. 3 we plot our data for the half of the chiral condensate and the Polyakov loop at $\alpha = 0.275$, which should be compared with the data in Fig. 1 where $\alpha = 0.2$.

IV. THE EFFECT OF THE 8-QUARK INTERACTION

We have briefly investigated on the role of other interactions on the entanglement of deconfinement and chiral symmetry restoration crossovers. We report here the results related to the effect of the 8-quark term, which has been extensively studied in [61] in relation to the vacuum stability of the NJL model, to the hadron properties and to the critical temperature at zero baryon density; besides, it has been studied in the context of the P-NJL model in [24, 31, 45]. To this end, we add to the interaction lagrangian in Eq. (2), the following term

$$G_8 \left[(\bar{\psi}\psi)^2 + (i\bar{\psi}\gamma_5\tau\psi)^2 \right]. \quad (23)$$

In principle, we expect that the constant G_8 acquires a dependence on the Polyakov loop as well; however, for simplicity we neglect this dependence here, since we are only interested to understand the qualitative effect of the interaction (23). We remark that the model studied in this Section is different from the P-NJL₈ model defined in [31]; in the latter, the dependence of G on L is neglected.

At the one-loop order we have

$$\mathcal{L} = -2\bar{u}u [G\Sigma + 2G_8\Sigma^3] - 2\bar{d}d [G\Sigma + 2G_8\Sigma^3] - 3G_8\Sigma^4 - G_S\Sigma^2, \quad (24)$$

instead of Eq. (6). The thermodynamic potential is still given by Eq. (17), with

$$U_M = 3G_8\Sigma^4 + G_S\Sigma^2, \quad (25)$$

and

$$M_u = M_d = m_0 + 2(G\Sigma + 2G_8\Sigma^3), \quad (26)$$

instead of Eq. (14). The parameters are fixed as in [45], that is $\Lambda = 589$ MeV, $g = 5 \times 10^{-6}$ MeV⁻², $G_8 = 6 \times 10^{-22}$ MeV⁻⁸ and $m_0 = 5.6$ MeV.

In Fig. 4 we plot our data for the chiral condensate and the expectation value of the Polyakov loop, as a function of temperature, for several values of the magnetic field strength and for $\alpha = 0.1$. We find that even at this smaller value of α , the two crossovers are entangled at large magnetic fields. On the other hand, we find that taking a running NJL coupling makes the crossovers sharper, and eventually we measure a discontinuity in the order parameters for a large magnetic field strength.

In Fig. 5 we plot the critical temperatures as a function of α , for $eB = 0$ and $eB = 19m_\pi^2$. At $eB = 0$ the two crossovers are entangled already at $\alpha = 0$; therefore, the effect of the entanglement vertex is to make the crossover sharper. Eventually, at the critical value $\alpha = 0.125$ the crossover is replaced by a sudden jump of the expectation values, analogously to the results that we find in the model without 8-quark term. As we increase eB , the deconfinement and chiral crossovers are split at $\alpha = 0$, in agreement with our previous findings [45]. However, the split in this case is more modest than the split that we measure in the model with $G_8 = 0$. In that case, at $eB = 19m_\pi^2$ we find a split of $\approx 30\%$, to be compared with the one that we read from Fig. 5 for the model with 8-quark interaction, namely $\approx 12\%$. Therefore, our conclusion is that the 8-quark interaction helps to keep the two crossovers close in a strong magnetic field, even if it is not enough and the entanglement vertex has to be included, as it is clear from Fig. 5.

V. THE PHASE DIAGRAM

In Fig. 6 we collect our data on the pseudo-critical temperatures for deconfinement and chiral symmetry restoration, in the form of a phase diagram in the $eB - T$ plane.

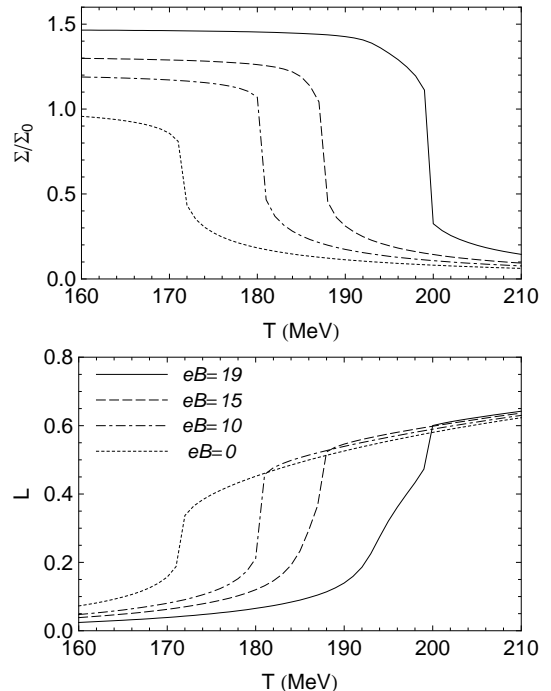


FIG. 4. *Upper panel:* Chiral condensate Σ , measured in units of the chiral condensate at zero temperature and zero field, Σ_0 , as a function of temperature, for several values of the magnetic field strength. *Lower panel:* Expectation value of the Polyakov loop P as a function of temperature, for several values of the magnetic field strength. The results are obtained within the model with 8-quark interaction and $\alpha = 0.1$. In the figures, the magnetic fields are measured in units of m_π^2 . Lines with the same dasheding correspond to the same value of the magnetic field strength.

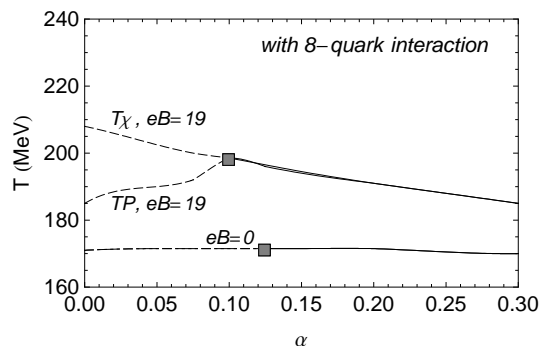


FIG. 5. Pseudo-critical temperatures as functions of the parameter α in the NJL coupling constant. Dashed lines correspond to the Polyakov loop crossover, for $eB = 0$ and $eB = 19$. Dot-dashed lines correspond to the chiral crossover. The grey squares denote the value of α at which the crossover becomes a first-order phase transition.

In the upper panel we show the results obtained within the EPNJL model; in the lower panel, we plot the results of the PNJL₈ model, that are obtained using the fitting functions computed in [45]. In the figure, the magnetic field is measured in units of m_π^2 ; temperature is measured in units of the deconfinement pseudo-critical temperature at zero magnetic field, namely $T_{B=0} = 185.5$ MeV for the EPNJL model, and $T_{B=0} = 175$ MeV for the PNJL₈ model. For any value of eB , we identify the pseudo-critical temperature with the peak of the effective susceptibility.

It should be kept in mind, however, that the definition of a pseudo-critical temperature in this case is not unique, because of the crossover nature of the phenomena that we describe. Other satisfactory definitions include the temperature at which the order parameter reaches one half of its asymptotic value (which corresponds to the $T \rightarrow 0$ limit for the chiral condensate, and to the $T \rightarrow +\infty$ for the Polyakov loop), and the position of the peak in the true susceptibilities. The expectation is that the critical temperatures computed in these different ways differ from each other only of few percent. This can be confirmed concretely using the data in Fig. 2 at $eB = 30m_\pi^2$. Using the peak of the effective susceptibility we find $T_\chi = 225$ MeV and $T_L = 224$ MeV; on the other hand, using the half-value criterion, we find $T_\chi = 227$ MeV and $T_L = 222$ MeV, in very good agreement with the previous estimate. Therefore, the qualitative picture that we derive within our simple calculational scheme, namely the entanglement of the two crossovers in a strong magnetic field, should not be affected by using different definitions of the critical temperatures.

Firstly we focus on the phase diagram of the EPNJL model, which is one of the novelties of our study. In the upper panel of Fig. 6, the dashed and dot-dashed lines correspond to the deconfinement and chiral symmetry restoration pseudo-critical temperatures, respectively. We have fit our data using the following functional form:

$$\frac{T_{\chi,L}(eB)}{T_c} = 1 + A \left(\frac{|eB|}{T_c^2} \right)^\alpha, \quad (27)$$

where the subscripts χ, L correspond to the (approximate) chiral restoration and deconfinement temperatures, respectively. The functional form is taken in analogy to the one used in [40]. Numerical values of the best-fit coefficients are collected in Table I. As a consequence of the entanglement, the two crossovers stay closed also in very strong magnetic field, as we have already discussed in the previous Sections. The grey region in the Figure denotes a phase in which quark matter is (statistically) deconfined, but chiral symmetry is still broken. According to [62, 63], we can call this phase as Constituent Quark Phase (CQP).

On the lower panel of Fig. 6 we have drawn the phase diagram for the PNJL₈ model; it is obtained using Eq. (27) with the coefficients computed in Ref. [45], and collected in Table I. The critical temperature at

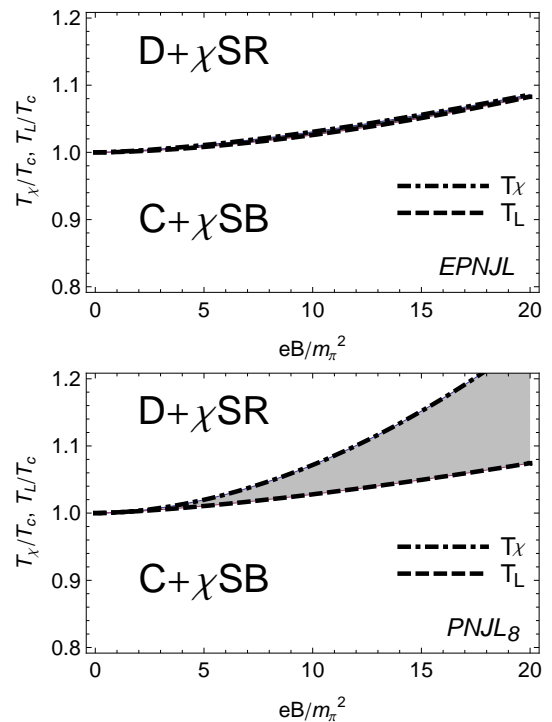


FIG. 6. *Upper panel:* Phase diagram in the $eB - T$ plane for the EPNJL model. Temperatures on the vertical axis are measured in units of the pseudo-critical temperature for deconfinement at $eB = 0$, namely $T_c = 185.5$ MeV. *Lower panel:* Phase diagram in the $eB - T$ plane for the PNJL₈ model. Temperatures on the vertical axis are measured in units of the pseudo-critical temperature for deconfinement at $eB = 0$, namely $T_c = 175$ MeV. In both the phase diagrams, T_χ, T_L correspond to the chiral and deconfinement pseudo-critical temperatures, respectively. The grey shaded region denotes the portion of phase diagram in which hot quark matter is deconfined and chiral symmetry is still broken spontaneously.

TABLE I. Coefficients of the fit function defined in Eq. (27) for the two models.

	A	α	T_c (MeV)
T_χ , EPNJL	2.34×10^{-3}	1.49	185.5
T_L , EPNJL	1.43×10^{-3}	1.68	185.5
T_χ , PNJL ₈ [45]	2.4×10^{-3}	1.85	175
T_L , PNJL ₈ [45]	2.1×10^{-3}	1.41	175

zero field in this case is a little smaller than the same temperature for the EPNJL model, because the parameters needed to fit the vacuum properties are different. However, a comparison among the two phase diagrams is still instructive. The most astonishing feature of the phase diagram of the PNJL₈ model is the entity of the split among the deconfinement and the chiral restoration crossover. The difference with the result of the EPNJL model is that in the former, the entanglement with the Polyakov loop is neglected in the NJL coupling constant.

As we have already mentioned in the previous Section, the maximum amount of split that we find within the EPNJL model, at the largest value of magnetic field considered here, is of the order of 2%; this number has to be compared with the split at $eB = 20m_\pi^2$ in the PNJL₈ model, namely $\approx 12\%$. The larger split causes a considerable portion of the phase diagram to be occupied by the CQP.

Keeping into account the crudeness of the two models, it is fair to say that they share one important feature: both deconfinement and chiral symmetry restoration temperature are increased by a strong magnetic field. They disagree quantitatively, in the sense that the amount of split in the EPNJL model is more modest in comparison with that obtained in the PNJL₈ model. Before closing, we notice that a similar phase diagram calculation has been performed within the Quark-Meson (QM in the following) model in [44]. In this reference, the magnetic field has the same effect that we measure in the PNJL₈ model, that is, to split of deconfinement and chiral symmetry restoration crossovers. Besides, both T_χ and T_L are enhanced by a magnetic field, in excellent agreement with the behavior that we find within the several NJL-like models that we have used in this study.

On the Lattice side, the most recent data about this kind of study are those of Ref. [40]. In these data, the split among the two crossovers is absent. Then the Lattice data seem to point towards the phase diagram of the EPNJL model. On the other hand, the results of [40] might not be definitive, in the sense that both the lattice size might be enlarged, and the pion mass could be lowered to its physical value in the vacuum. Therefore, it will be interesting to compare our results with more refined data.

VI. CONCLUSIONS

In this article, we have studied chiral symmetry restoration and deconfinement in a strong magnetic background, using an effective model of QCD. In particular, we have reported our results about the effect of the entangled vertex on the phase diagram. Our main result is that the entanglement reduces considerably the split among the deconfinement and the chiral symmetry crossovers studied in [43–45], as expected.

We have also studied the effect of the 8-quark term on the split. Our results suggest that the 8-quark interaction helps the two crossovers to be close. Furthermore, we have shown that the crossovers become sharper and then they are replaced by a sudden jump of the expectation values, as the value of α in the entanglement vertex is larger than a critical value.

We have then compared our results with those of other model calculations, namely the PNJL model [43], the Quark-Meson model [44] and the PNJL₈ model [45]. The most striking similarity among the several models is that they all support the scenario in which chiral symme-

try restoration and deconfinement temperatures are enhanced by a strong magnetic field. The models differ quantitatively for the amount of split measured (very few percent for the EPNJL model, and of the order of 10% for the other models for $eB \approx 20m_\pi^2$).

Furthermore, we have compared our results with those obtained on the Lattice [40]. In [40], the largest value of magnetic field considered is $eB \approx 0.75 \text{ GeV}^2$, which corresponds to $eB/m_\pi^2 \approx 38$. The Lattice data seem to point towards the phase diagram of the EPNJL model. On the other hand, the results of [40] might not be definitive: the lattice size might be enlarged, the lattice spacing could be taken smaller (in [40] the lattice spacing is $a = 0.3 \text{ fm}$), and the pion mass could be lowered to its physical value in the vacuum. As a consequence, it will be interesting to compare our results with more refined data in the future.

This comparison can be interesting also for another reason. Indeed, the EPNJL model and the PNJL₈ can describe the same QCD thermodynamics at zero and imaginary quark chemical potential [31], but they differ qualitatively for the interaction content. As we have shown, they have some quantitative discrepancy for what concerns the response to a strong magnetic field. Therefore, more refined Lattice data in magnetic field might help to discern which of the two models is a more faithful description of QCD.

From our point of view, it is fair to admit that our study might have a weak point, namely, we miss a microscopic computation of the parameters α_1, α_2 in Eq. (5). For concreteness, we have used the best-fit values quoted in [31], showing in addition that changing the value of T_0 in the Polyakov loop effective potential as in [31], we obtain $T_\chi = T_L = 175 \text{ MeV}$, in excellent agreement with that reference. This is comforting, since it shows that our different UV-regulator does not affect the qualitative result at zero field, namely the coincidence of T_χ and T_L . Besides, we are aware that Eq. (5) is just a particular choice of the functional dependence of the NJL coupling constant on the Polyakov loop expectation value. Different functional forms respecting the C and the extended Z_3 symmetry are certainly possible, and without a rigorous derivation of Eq. (5) using functional renormalization group techniques as suggested in [37], it merits to study our problem using different choices for $G(L)$ in the next future. For these reasons, we prefer to adopt a conservative point of view: it is interesting that a model which is adjusted in order to reproduce Lattice data at zero and imaginary chemical potential, predicts that the two QCD transitions are entangled in a strong magnetic background; however, this conclusion might not be definitive, since there exist other model calculations which share a common basis with ours, and which show a more pronounced split of the QCD transitions in a strong magnetic background. More refined Lattice data will certainly help to discern which of the two scenarios is the most favorable.

As a natural continuation of this work, it is worth to

perform the computation of the chiral magnetization [41] at finite temperature. Besides, the technical machinery used here can be easily applied to a microscopic study of the spectral properties of mesons in strong magnetic field. In this direction, it is interesting to compute the masses of the charged ρ -mesons at low temperature, in order to investigate their condensation at large magnetic field as suggested in [48]. Furthermore, it would be interesting to make a complete (analytical or semi-analytical) study of the chiral limit, to estimate the effect of the magnetic field on the universality class of two-flavor QCD. We will report on these topics in the next future.

ACKNOWLEDGMENTS

We acknowledge E. Cartman, M. Cristoforetti, A. Flachi, K. Fukushima, F. Greco, E. M. Ilgenfritz, T. Kahara, K. I. Kondo, V. Mathieu and H. Warringa, for valuable discussions and encouraging comments about the topics discussed in this article. Besides, we acknowledge E. Fraga, A. Mizher and A. Ohnishi for a careful reading of the manuscript. Moreover, we acknowledge many discussions and heavy correspondence with M. Chernodub, M. D'Elia and M. Frasca. We also thank T. Kunihiro for comments about the effects of the 8-quark term on the phase transitions. The work of M. R. is supported by JSPS under the contract number P09028. The numerical calculations were carried out on Altix3700 BX2 at YITP in Kyoto University.

-
- [1] P. de Forcrand and O. Philipsen, JHEP **0701**, 077 (2007); JHEP **0811**, 012 (2008); PoS **LATTICE2008**, 208 (2008).
 - [2] Y. Aoki, S. Borsanyi, S. Durr, Z. Fodor, S. D. Katz, S. Krieg and K. K. Szabo, JHEP **0906**, 088 (2009); S. Borsanyi *et al.*, arXiv:1007.2580 [hep-lat].
 - [3] A. Bazavov *et al.*, Phys. Rev. D **80**, 014504 (2009).
 - [4] M. Cheng *et al.*, Phys. Rev. D **81**, 054510 (2010).
 - [5] F. Karsch, E. Laermann and A. Peikert, Nucl. Phys. B **605**, 579 (2001); F. Karsch, Lect. Notes Phys. **583**, 209 (2002); O. Kaczmarek and F. Zantow, Phys. Rev. D **71**, 114510 (2005).
 - [6] C. S. Fischer, Phys. Rev. Lett. **103**, 052003 (2009); C. S. Fischer and J. A. Mueller, Phys. Rev. D **80**, 074029 (2009); C. S. Fischer, A. Maas and J. A. Muller, Eur. Phys. J. C **68**, 165 (2010).
 - [7] A. C. Aguilar and J. Papavassiliou, arXiv:1010.5815 [hep-ph].
 - [8] C. Wetterich, Phys. Lett. B **301**, 90 (1993).
 - [9] C. Feuchter and H. Reinhardt, Phys. Rev. D **70**, 105021 (2004); Phys. Rev. D **71**, 105002 (2005).
 - [10] M. Leder, J. M. Pawłowski, H. Reinhardt and A. Weber, arXiv:1006.5710 [hep-th].
 - [11] J. Braun, Eur. Phys. J. C **64**, 459 (2009) [arXiv:0810.1727 [hep-ph]].
 - [12] J. Braun, L. M. Haas, F. Marhauser and J. M. Pawłowski, arXiv:0908.0008 [hep-ph].
 - [13] M. Frasca, Phys. Lett. B **670**, 73 (2008); Mod. Phys. Lett. A **24** (2009) 2425; arXiv:1007.4479 [hep-ph].
 - [14] Y. Nambu and G. Jona-Lasinio, Phys. Rev. **122**, 345 (1961); Y. Nambu and G. Jona-Lasinio, Phys. Rev. **124**, 246 (1961).
 - [15] U. Vogl and W. Weise, Prog. Part. Nucl. Phys. **27**, 195 (1991); S. P. Klevansky, Rev. Mod. Phys. **64**, 649 (1992); T. Hatsuda and T. Kunihiro, Phys. Rept. **247**, 221 (1994); M. Buballa, Phys. Rept. **407**, 205 (2005).
 - [16] A. M. Polyakov, Phys. Lett. B **72**, 477 (1978); L. Susskind, Phys. Rev. D **20**, 2610 (1979); B. Svetitsky and L. G. Yaffe, Nucl. Phys. B **210**, 423 (1982); B. Svetitsky, Phys. Rept. **132**, 1 (1986).
 - [17] P. N. Meisinger and M. C. Ogilvie, Phys. Lett. B **379**, 163 (1996).
 - [18] K. Fukushima, Phys. Lett. B **591**, 277 (2004).
 - [19] C. Ratti, M. A. Thaler and W. Weise, Phys. Rev. D **73**, 014019 (2006).
 - [20] S. Roessner, C. Ratti and W. Weise, Phys. Rev. D **75**, 034007 (2007).
 - [21] E. Megias, E. Ruiz Arriola and L. L. Salcedo, Phys. Rev. D **74**, 114014 (2006); Eur. Phys. J. A **31**, 553 (2007).
 - [22] C. Sasaki, B. Friman and K. Redlich, Phys. Rev. D **75**, 074013 (2007).
 - [23] S. K. Ghosh, T. K. Mukherjee, M. G. Mustafa and R. Ray, Phys. Rev. D **77**, 094024 (2008).
 - [24] A. Bhattacharyya, P. Deb, S. K. Ghosh and R. Ray, Phys. Rev. D **82**, 014021 (2010).
 - [25] K. Fukushima, Phys. Rev. D **77**, 114028 (2008) [Erratum-ibid. D **78**, 039902 (2008)]; M. Ciminale, R. Gatto, N. D. Ippolito, G. Nardulli and M. Ruggieri, Phys. Rev. D **77**, 054023 (2008); W. j. Fu, Z. Zhang and Y. x. Liu, Phys. Rev. D **77**, 014006 (2008); T. Hell, S. Roessner, M. Cristoforetti and W. Weise, Phys. Rev. D **81**, 074034 (2010).
 - [26] H. Abuki, R. Anglani, R. Gatto, G. Nardulli and M. Ruggieri, Phys. Rev. D **78**, 034034 (2008).
 - [27] Y. Sakai, K. Kashiwa, H. Kouno and M. Yahiro, Phys. Rev. D **77**, 051901 (2008); Phys. Rev. D **78**, 036001 (2008).
 - [28] Y. Sakai, K. Kashiwa, H. Kouno, M. Matsuzaki and M. Yahiro, arXiv:0902.0487 [hep-ph].
 - [29] H. Abuki, M. Ciminale, R. Gatto, N. D. Ippolito, G. Nardulli and M. Ruggieri, Phys. Rev. D **78**, 014002 (2008).
 - [30] K. Kashiwa, H. Kouno, M. Matsuzaki and M. Yahiro, Phys. Lett. B **662**, 26 (2008).
 - [31] Y. Sakai, T. Sasaki, H. Kouno and M. Yahiro, Phys. Rev. D **82**, 076003 (2010).
 - [32] T. Hell, S. Roessner, M. Cristoforetti and W. Weise, Phys. Rev. D **79**, 014022 (2009).
 - [33] T. K. Herbst, J. M. Pawłowski and B. J. Schaefer, arXiv:1008.0081 [hep-ph].
 - [34] V. Skokov, B. Friman and K. Redlich, arXiv:1008.4570 [hep-ph].
 - [35] T. Kahara and K. Tuominen, Phys. Rev. D **78**, 034015 (2008); T. Kahara and K. Tuominen, Phys. Rev. D **80**, 114022 (2009); T. Kahara and K. Tuominen,

- arXiv:1006.3931 [hep-ph].
- [36] T. L. Partyka and M. Sadzikowski, arXiv:1011.0921 [hep-ph].
 - [37] K. I. Kondo, Phys. Rev. D **82**, 065024 (2010).
 - [38] K. Langfeld, C. Kettner and H. Reinhardt, Nucl. Phys. A **608**, 331 (1996) [arXiv:hep-ph/9603264].
 - [39] M. Frasca, arXiv:0803.0319 [hep-th]; arXiv:1002.4600 [hep-ph].
 - [40] M. D'Elia, S. Mukherjee and F. Sanfilippo, Phys. Rev. D **82**, 051501 (2010).
 - [41] P. V. Buividovich, M. N. Chernodub, E. V. Luschevskaya and M. I. Polikarpov, Phys. Rev. D **81**, 036007 (2010); Phys. Lett. B **682**, 484 (2010); Nucl. Phys. B **826**, 313 (2010).
 - [42] P. Cea and L. Cosmai, JHEP **0302**, 031 (2003); P. Cea and L. Cosmai, JHEP **0508**, 079 (2005); P. Cea, L. Cosmai and M. D'Elia, JHEP **0712**, 097 (2007).
 - [43] K. Fukushima, M. Ruggieri and R. Gatto, Phys. Rev. D **81**, 114031 (2010).
 - [44] A. J. Mizher, M. N. Chernodub and E. S. Fraga, Phys. Rev. D **82**, 105016 (2010).
 - [45] R. Gatto and M. Ruggieri, Phys. Rev. D **82**, 054027 (2010).
 - [46] S. P. Klevansky and R. H. Lemmer, Phys. Rev. D **39**, 3478 (1989); H. Suganuma and T. Tatsumi, Annals Phys. **208**, 470 (1991); I. A. Shushpanov and A. V. Smilga, Phys. Lett. B **402**, 351 (1997); D. N. Kabat, K. M. Lee and E. J. Weinberg, Phys. Rev. D **66**, 014004 (2002); T. Inagaki, D. Kimura and T. Murata, Prog. Theor. Phys. **111**, 371 (2004); T. D. Cohen, D. A. McGady and E. S. Werbos, Phys. Rev. C **76**, 055201 (2007); V. P. Gusynin, V. A. Miransky and I. A. Shovkovy, Nucl. Phys. B **462**, 249 (1996); Nucl. Phys. B **563**, 361 (1999); G. W. Semenoff, I. A. Shovkovy and L. C. R. Wijewardhana, Phys. Rev. D **60**, 105024 (1999); V. A. Miransky and I. A. Shovkovy, Phys. Rev. D **66**, 045006 (2002); K. G. Klimenko, Theor. Math. Phys. **89**, 1161 (1992) [Teor. Mat. Fiz. **89**, 211 (1991)]; K. G. Klimenko, Z. Phys. C **54**, 323 (1992); K. G. Klimenko, Theor. Math. Phys. **90**, 1 (1992) [Teor. Mat. Fiz. **90**, 3 (1992)]; B. Hiller, A. A. Osipov, A. H. Blin and J. da Providencia, SIGMA **4**, 024 (2008); N. O. Agasian and S. M. Fedorov, Phys. Lett. B **663**, 445 (2008); E. S. Fraga and A. J. Mizher, Phys. Rev. D **78**, 025016 (2008).
 - [47] L. Campanelli and M. Ruggieri, Phys. Rev. D **80**, 034014 (2009).
 - [48] M. N. Chernodub, Phys. Rev. D **82**, 085011 (2010).
 - [49] I. E. Frolov, V. C. Zhukovsky and K. G. Klimenko, Phys. Rev. D **82**, 076002 (2010).
 - [50] O. Bergman, G. Lifschytz and M. Lippert, JHEP **0805**, 007 (2008); C. V. Johnson and A. Kundu, JHEP **0812**, 053 (2008); A. V. Zayakin, JHEP **0807**, 116 (2008).
 - [51] D. E. Kharzeev, L. D. McLerran and H. J. Warringa, Nucl. Phys. A **803**, 227 (2008).
 - [52] V. Skokov, A. Y. Illarionov and V. Toneev, Int. J. Mod. Phys. A **24**, 5925 (2009).
 - [53] P. V. Buividovich, M. N. Chernodub, E. V. Luschevskaya and M. I. Polikarpov, Phys. Rev. D **80**, 054503 (2009); M. Abramczyk, T. Blum, G. Petropoulos and R. Zhou, PoS **LAT2009**, 181 (2009).
 - [54] M. D'Elia and F. Sanfilippo, Phys. Rev. D **80**, 111501 (2009).
 - [55] C. Bonati, G. Cossu, M. D'Elia and F. Sanfilippo, arXiv:1011.4515 [hep-lat].
 - [56] V. I. Ritus, Annals Phys. **69**, 555 (1972); C. N. Leung and S. Y. Wang, Nucl. Phys. B **747**, 266 (2006).
 - [57] E. Elizalde, E. J. Ferrer and V. de la Incera, Annals Phys. **295**, 33 (2002); E. Elizalde, E. J. Ferrer and V. de la Incera, Phys. Rev. D **70**, 043012 (2004).
 - [58] E. J. Ferrer, V. de la Incera and C. Manuel, Phys. Rev. Lett. **95**, 152002 (2005); E. J. Ferrer, V. de la Incera and C. Manuel, Nucl. Phys. B **747**, 88 (2006).
 - [59] K. Fukushima and H. J. Warringa, Phys. Rev. Lett. **100**, 032007 (2008); J. L. Noronha and I. A. Shovkovy, Phys. Rev. D **76**, 105030 (2007).
 - [60] K. Fukushima, D. E. Kharzeev and H. J. Warringa, Nucl. Phys. A **836**, 311 (2010).
 - [61] A. A. Osipov, B. Hiller and J. da Providencia, Phys. Lett. B **634**, 48 (2006); A. A. Osipov, B. Hiller, A. H. Blin and J. da Providencia, Annals Phys. **322**, 2021 (2007); A. A. Osipov, B. Hiller, J. Moreira, A. H. Blin and J. da Providencia, Phys. Lett. B **646**, 91 (2007); A. A. Osipov, B. Hiller, J. Moreira and A. H. Blin, Phys. Lett. B **659**, 270 (2008); B. Hiller, J. Moreira, A. A. Osipov and A. H. Blin, Phys. Rev. D **81**, 116005 (2010).
 - [62] J. Cleymans, K. Redlich, H. Satz and E. Suhonen, Z. Phys. C **33**, 151 (1986).
 - [63] H. Kouno and F. Takagi, Z. Phys. C **42**, 209 (1989).